Towards the Development of a Spatial Decision Support System (SDSS) for the Application of Climate Forecasts in Uruguayan Rice Production Sector

A. Roel · W. E. Baethgen

10.1 Introduction

Recent scientific advancements are improving the ability to predict some major elements of climate variability, in advance of the crop-growing season. In selected regions of the world, climate anomalies are linked to the onset and intensity of a warm or cold event of the El Niño-Southern Oscillation (ENSO) phenomenon. Southeast of South America is within the regions of influence of this phenomenon (Ropelewski and Halpert 1989). Hence seasonal weather and climate fluctuations have significant economical impacts on the agricultural production sector of this region.

More recent studies conducted in southeastern South America revealed the existence of a near symmetry between impacts of El Niño and La Niña on precipitation as well as on non-irrigated crop productivity. Positive rainfall anomalies prevail in El Niño years, and negative rainfall anomalies prevail in La Niña years, during the austral spring and/or summer months (Baethgen 1997; Baethgen and Giménez 2002).

While there has been much written about impacts of climate variability, there has been relatively little done in relation to applying knowledge of inherently imprecise climate predictions to modify actions ahead of likely impacts, i.e. applications of climate predictions. Although forecasts make predictions of climate variable behaviors for large regions of the world, these regions are not uniform. Hence in many situations in some areas of these regions forecast recommendations were suitable while in others they were not. A pilot project was then proposed to evolve a system for the effective application of a seasonal climate forecast, which can address the natural spatial variability in growing conditions that control productivity in a rice ecosystem in Uruguay.

Therefore the objectives of this study were: (1) evaluate ENSO effects on Uruguayan rice production; (2) evaluate the capability of crop simulation models in recreating the observed yield spatial variability; and (3) simulate rice yield spatial variability under different seasonal forecast scenarios: El Niño, La Niña and neutral years.

10.2 Materials and Methods

In this study, the relationship between ENSO 3.4 average total sea surface temperatures (SST) anomalies in October, November and December (OND) and rice yield have been analyzed to evaluate ENSO effects on Uruguayan rice production. Yield data were obtained from the Uruguayan Rice Growers Association (ACA). Yields for any given year were expressed as the relative difference between the observed yield for that year and the yield predicted by the regression model (Eq. 10.1):

$$RYD = (Yld(n) - PYld(n)) \cdot 100 / PYld(n) \quad (10.1)$$

where, RYD = relative yield deviation expressed in (%), $Yld(n)$ = observed crop yield for year n, and $PYld(n)$ = yield predicted by regression model for year n.

SST anomalies were obtained from the Climate Prediction Center of NOAA. The anomalies were calculated relative to the period 1950–2003 and aggregated into three-month period means. Rice is normally planted during October–November and harvested during the end of March through May. Therefore any possible relationships found during OND may have significant forecasting applications for this crop.

The study was conducted at a 12 ha rice field located at El Paso de la Laguna Experimental Unit of the National Institute of Agricultural Research (INIA), Uruguay. The cultivar used was El Paso 144 and the planting date was 7–8 November 2002. Seeding rate was 190 kg ha^{-1}. Rice was direct seeded on dry soil. Fertilizer applications were: 170 kg ha^{-1} 15-35-15 (N-P-K) at planting followed by 50 kg ha^{-1} of urea at flooding time (30 days after emergence) and 50 kg ha^{-1} of urea at panicle initiation.

Ten locations were selected in this 12 ha rice field in which recording data loggers (Hobo H8 Pro) were fitted. These loggers have an internal temperature sensor that measures ambient air temperature, in this situation representative of canopy temperature, and an external sensor that was used to measure water temperature. The loggers were attached to stakes placed vertically in the field, with the external sensors placed approximately 0.05 m below field water level. As the rice grew, the internal sensors were moved upward along the stake so that they were always near the top of the canopy. Water and canopy temperatures were measured hourly throughout the growing season. Data logger locations were georeferenced using a back-pack differential global positioning systems (DGPS) receiver (Trimble AG 132).

Daily rainfall, temperature and solar radiation data were obtained from the Agrometeorological Weather Station located at El Paso de la Laguna Experimental Unit of the INIA for the period 1973–2003.

At harvest, yield, yield components, and percent blanking were recorded in the vicinity of each sensor. Sensors were removed before harvest. A sample plot (2.5 m × 3.5 m) was harvested with an experimental plot combine at each sensor location. Yields standardized to 14% moisture content were measured. Interpolated yield maps of the field were created using a geographic information system (Arcview, ESRI, Redlands, CA). Yield data from each of the ten locations were spatially interpolated to a fixed 5 m × 5 m grid using inverse distance weighted interpolation with power 2 and number of neighbors 12.

Soil samples were extracted at three different depths: 0–10 cm, 10–20 cm and 20–30 cm at the same locations where sensors were installed. Yield was predicted at each sensor locations using the DSSAT v3.5 CERES-Rice model.

10.3 Results and Discussion

10.3.1 ENSO Effects on Uruguayan Rice Production

The fact that rice is irrigated under Uruguayan conditions theoretically should ameliorate ENSO effects on this crop productivity. Straightforward reasoning will indi-

cate that for an irrigated crop like rice, ENSO phases can have opposite effects than in non-irrigated ones.

Figure 10.1 shows national rice yield average evolution in the last 31 growing seasons (1972–2003). In order to analyze ENSO impacts on rice production the probabilistic impact of ENSO phases on the distribution shifts of crop yields were studied using the same approach as the one used by Baethgen. The detrended national yield crop average data from 1973 to 2003 were divided into quartiles and any given value was defined as being "high" if it was greater than the third quartile (upper 75% of the data), "low" if it was less than the first quartile (lower 25%), and "normal" if its value fell between the first and the third quartile (central 50% of the data). By this way the range of average yield values that corresponded to each quartile were determined. Using these values the shift in the distribution of crop yields were studied for the different ENSO phases (El Niño, La Niña and neutral). The IRI classification of El Niño, neutral and La Niña years was used (*http://iri.columbia.edu/climate/ENSO/enso.html*).

Table 10.1 shows the classification of the series of years according to ENSO phases. This analysis showed that the distribution of national relative yield differences (RYD) varied with ENSO phases (Fig. 10.2). For example, the frequency of high rice yield differences was more than two times higher in La Niña years than in neutral years. On the other hand in El Niño years the chances of having high yields were zero. In summary this figure clearly shows that in La Niña years the chance of having high yields increased with respect to the neutral years, while in El Niño years this chance strictly does not exist.

10.3.2 Spatial Variability

The DSSAT v3.5 rice model requires information about: weather (temperature and solar radiation), soil variables, genetic coefficients and crop management. Crop manage-

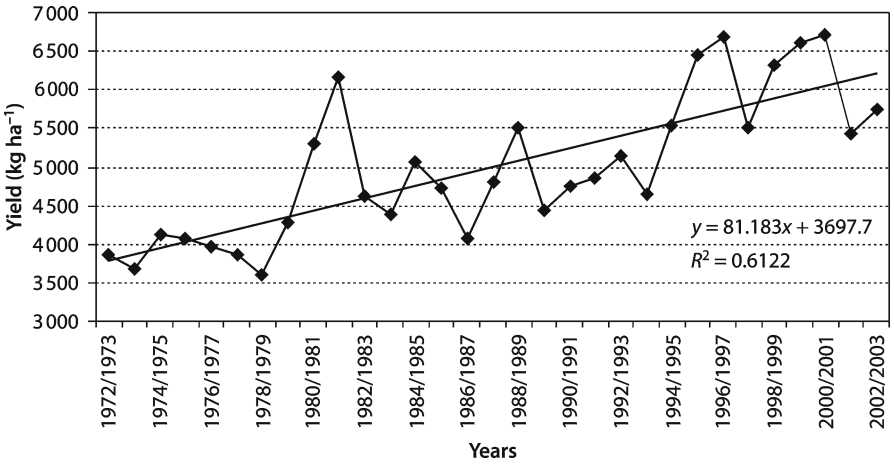

Fig. 10.1. National rice yield (1972–2002)

Table 10.1. El Niño, La Niña and neutral years

El Niño	Year	La Niña	Year	Neutral	Year
1972–1973	1	1973–1974	1	1978–1979	1
1976–1977	2	1974–1975	2	1979–1980	2
1977–1978	3	1975–1976	3	1980–1981	3
1982–1983	4	1984–1985	4	1981–1982	4
1986–1987	5	1988–1989	5	1983–1984	5
1987–1988	6	1995–1996	6	1985–1986	6
1990–1991	7	1998–1999	7	1989–1990	7
1991–1992	8	1999–2000	8	1993–1994	8
1992–1993	9	2000–2001	9	1996–1997	9
1994–1995	10			2001–2002	10
1997–1998	11			2002–2003	11

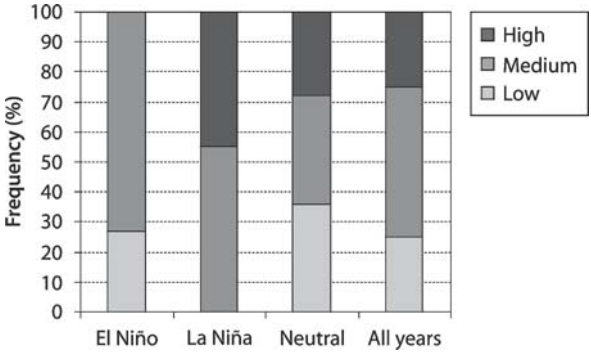

Fig. 10.2. National rice yield distribution and ENSO phases (1972–2003)

ment and genetic coefficients were uniform for the field since the same cultivar and management practices were applied throughout the studied field. In order to assess the capability of the model in recreating the observed rice yield spatial variability, three different simulations were carried out at each sensor location:

Simulation 1. Weather information (temperature and solar radiation) was extracted from the agrometeorological weather station located at INIA. Soil information was gathered from the soil analyses data that come from the samples extracted at each sensor location. In these simulations all locations have the same weather data but differ in the soil variables data.

Simulation 2. Same as above, but the temperature from the weather station was substituted with each canopy temperature's data registered at each sensor locations. In these simulations each location had its own temperature and soil data and shared the solar radiation data extracted from the weather station.

Simulation 3. Same as Simulation 2, but temperature from the weather station, was substituted with each water temperature data registered at each sensor locations.

Table 10.2 displays the correlation values between observed and simulated yields for all three simulations. Figure 10.3 displays the observed and interpolated predicted yield values for all simulations. In these figures, it can be observed that the crop simulation model was able to capture satisfactorily the spatial variability that was measured in the field. It is important to highlight in these figures that the actual observed spatial variation in yield ranges from 5 000 to 7 100 kg ha^{-1} (2 100 kg), while the predicted ones vary in general from 4 000–5 250 kg ha^{-1}. This indicates that the model tends to underestimate productivity under these conditions and that the observed spatial variability was indeed larger that what was predicted. The reason for this underprediction should be further investigated.

Table 10.2. Correlation between observed and predicted yield values

Simulation no.	Correlation with observed yield
1	0.80[a]
2	0.78[a]
3	0.90[a]

[a] $P = 0.0001$.

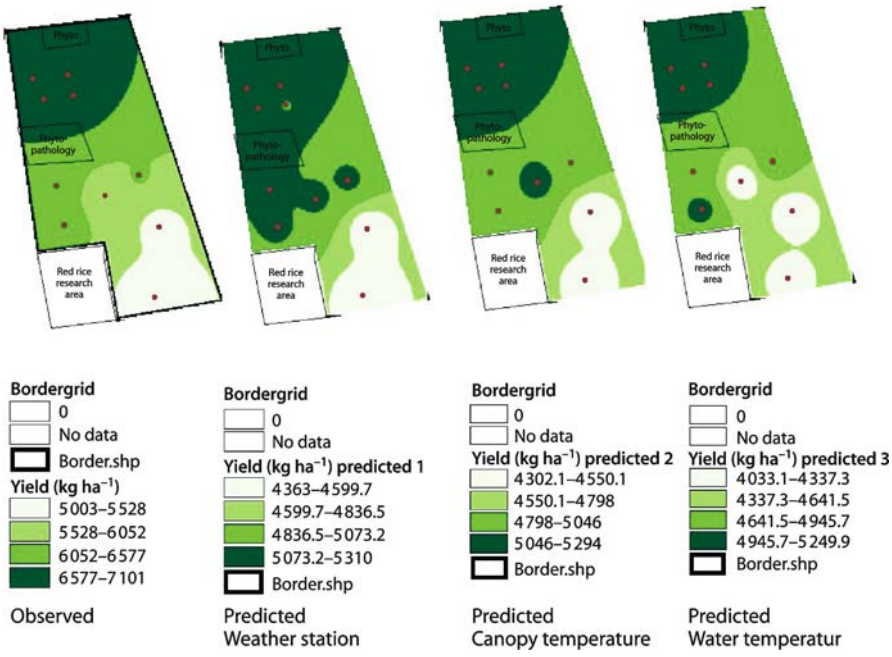

Fig. 10.3. Observed and predicted yield spatial variability for simulations 1–3

10.3.3
Temporal Variability

In order to achieve this, the average simulated yields of the 10 selected locations in the field were compared with the country's national rice yield average evolution in the last 16 growing seasons (1987–1988 to 2002–2003) (Fig. 10.4). For each growing season, the national rice yield average is determined by a large number of environmental situations (i.e. planting dates, fertilization, soils, cultivars, etc.). Differences among growing seasons are caused in part by the differences in the "average" climatic conditions of each growing season. In other words, each growing season can be classified as good or bad from the climatic point of view. The goal of this section of the study was to test if the model was able to capture those good, fair and bad years.

Overall the DSSAT v3.5 CERES-Rice model was able to capture satisfactorily rice yield temporal variability. The model was able to simulate higher or lower production levels in "good" or "bad" growing seasons. The only exceptions of the latter are in the 1990–1991 and 1998–1999 growing seasons when the model determined average yields for the field for these years were lower than in the previous seasons (1989–1990 and 1997–1998) when the national yield averages actually increased during these years with respect to the previous ones.

10.3.4
Spatiotemporal Variability

The model was run, in each of the ten selected locations in the field using the weather data from a series of years (1972–2003) to characterize the spatiotemporal variability. The same soil data, management practices (planting date, seeding rate, fertilization, etc.) and genetic data (El Paso 144) that were used in the studied field for 2002–2003 growing season were applied at each of the ten locations through out all of these years. Specific attention was given to evaluating if different regions within the studied field would react differentially to a given climatic data. Simulated yield data from each of the ten locations and for each 31 growing seasons were spatially interpolated in order to generate yield maps for each growing seasons. Figure 10.5 shows the set of yield maps

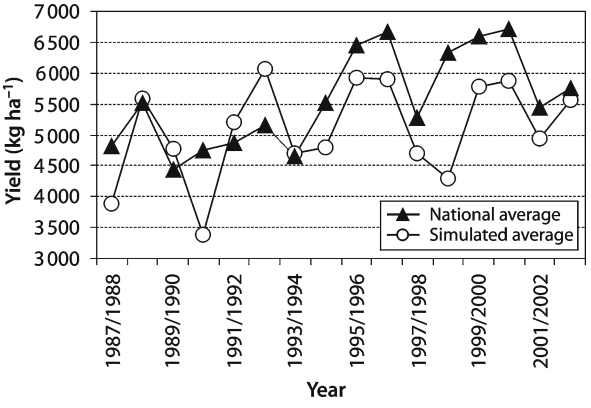

Fig. 10.4. National vs. simulated yields

from the 1972–1973 through the 2002–2003 growing seasons. In order to be able to display the yield range variability along these 31 growing seasons with a common legend, the whole data set of yield outcomes were and divided into quartiles. These quartiles defined the range of variability of the different yield classes displayed in Fig. 10.5.

Figure 10.5 also categorizes each growing season according to ENSO conditions (El Niño, La Niña and neutral conditions, Table 10.1). This figure shows that in all the growing seasons in which some part of the field presented production levels that fell in the lowest yield class (2 968–3 819 kg ha^{-1}, red color), those years corresponded to El Niño years (1986–1987, 1987–1988 and 1990–1991). Conversely in all the years classified as La Niña, the yield variation of the field tended to be in the highest yield classes (green and blue) with the exception of the 1998–1999 and 1974–1975 growing seasons. These results coincide with the previous ones suggesting that La Niña year's climatic conditions are better for rice production.

10.4 Conclusions

The availability of new technologies like yield monitors, yield mapping software, GPS, satellite and aerial images and GIS has made possible to measure crop growing conditions as well as grain yield within a field at a very high spatial resolution, allowing very fine and precise description of the spatial variability (Roel and Plant 2004). A number of research groups around the globe are seeking to apply seasonal climate forecasts to improve management of food production systems and security of farmer livelihood in the face of climatic risk. One of the tools frequently employed by these efforts is dynamic crop simulation models (Hansen 2000). In this study we integrate this tool with the mentioned advancements regarding the capability of a precise description of yield spatial variability. We consider that this integration may increase the possibility to evaluate the application of seasonal climate forecasts at a regional scale. This integration will allow to study if in fact regions within the scale at which climate prediction model output are given, react uniformly to different climatic conditions. Consequently, evaluations can be made as to whether uniform recommendations can be made from a given forecast or if certain areas within the scale of the forecast should be treated differently.

This study showed that the distribution of national rice yield averages varied with ENSO phases (Fig. 10.2). The frequency of high national rice yields average was more than two times higher in La Niña years than in neutral years. The study conducted in the 12 ha rice field showed that this field presented certain yield spatial pattern with high yielding areas at the north and center portion of the field and a low yielding areas at the south portion of the field. The DSSAT v3.5 CERES-Rice model showed to be able to capture satisfactorily rice yield variability at the spatial and temporal levels. When the model was run spatially, at the different locations within the field and temporally along the different growing seasons, the same pattern of low yield spatial variation can be observed in the southern part of the field. Overall, this suggests that there is no interaction between temporal and spatial effects, there were no climatic conditions (temporal variability) that can make that the south portion of the field achieve a higher yield than the northern portion.

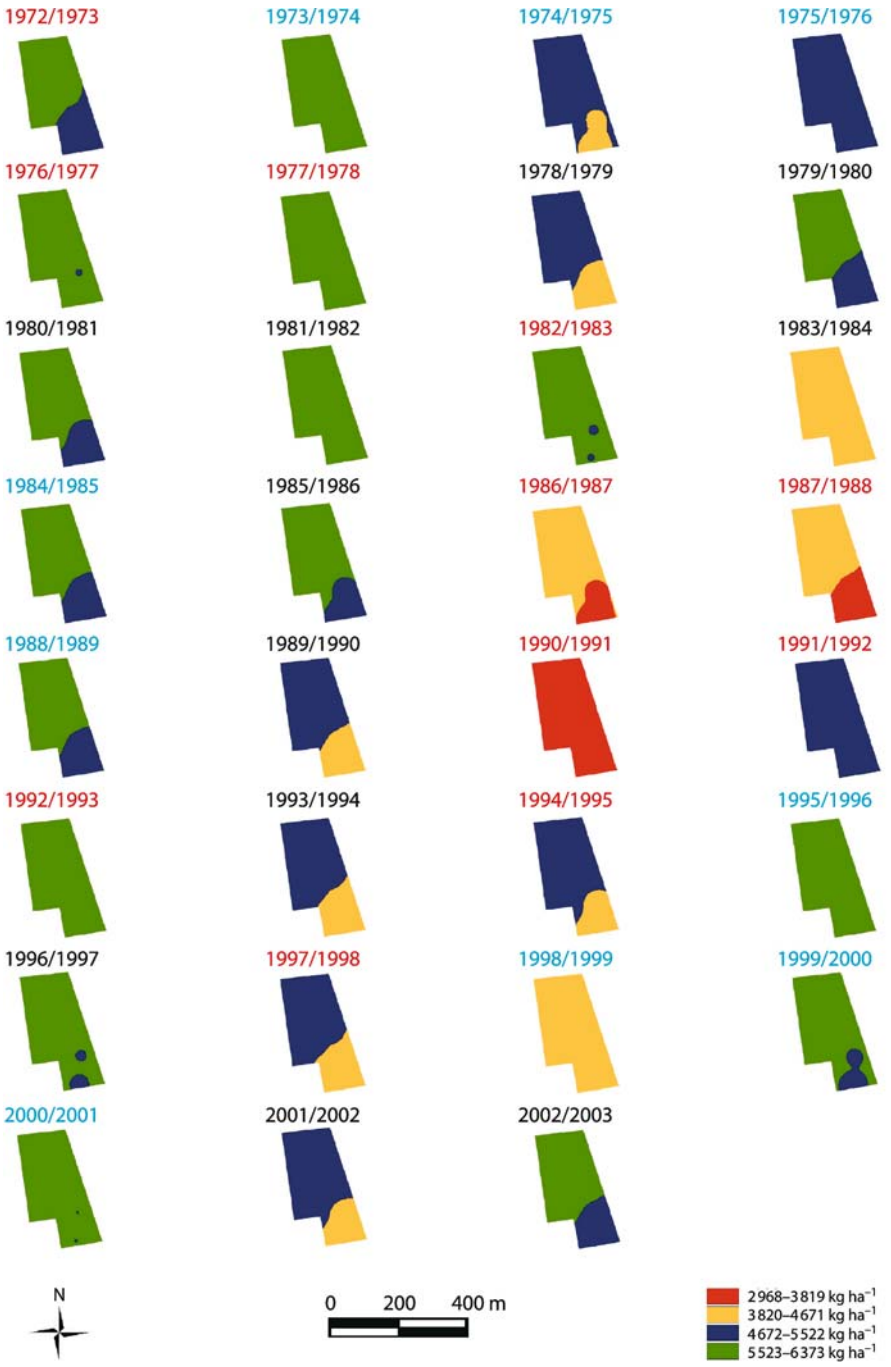

Fig. 10.5. Yield spatial variability; *red years* correspond to El Niño, *blue years* correspond to La Niña and *black years* to neutral conditions

The chief difficulty in linking climate forecasts scenarios with crop simulation models is the substantial mismatch between the forecast output spatial and temporal scales and crop simulation model input requirements. This study was able to demonstrate that for this rice field although we were able to characterize its yield spatial variability very precisely this pattern of spatial variability did not change with different climatic conditions. Therefore, yield spatial variability within this field seems to be regulated by factors related to the soil and not with the climatic conditions. Consequently, at the scale of this field forecast output scale did not constitute a problem. We believe that the approach used in this study can be implemented at a larger spatial scale to evaluate at which level of spatial resolution forecast output scale starts to become a problem.

References

Baethgen W (1997) Relaciones entre la temperatura superficial del Pacífico tropical y los rendimientos de cultivos en Uruguay. Workshop and Conference on the 1997-98 El Niño: Impacts and Potential Applications of Climate Prediction in Southeast South America, December 1997, Montevideo, Uruguay

Baethgen W, Giménez A (2002) Seasonal climate forecasts and the agricultural sector of Uruguay (*http://iri.columbia.edu/climate/ENSO/societal/resource/example/Baethgen.html*)

Hansen J (2000) Summary report of the workshop "Linking Climate Prediction Model Output with Crop Model Requirements", 28–29 April2000, Palisades, New York (IRI Publication CW/00/2)

Roel A, Plant R (2004) Spatiotemporal analysis of rice yield variability in two California rice fields. Agron J 96:77–90

Ropelewski CF, Halpert MS (1989) Precipitation patterns associated with high index phase of Southern Oscillation. J Climate 2:268–284